Fprint-97-001-1

2)

Charge-Coupled Devices as X-ray and Optical Sensors

J.A. Nousek, M.W. Bautz, B.E. Burke,
J.A. Gregory, R.E. Griffiths, R.L.
Kraft, H.L. Kwok, D.H. Lumb

FERMILAB
SEP 4 1997
LIBRARY

To appear in the CRC Handbook on Measurement, Instrumentation and Sensors.

Charge-Coupled Devices as X-ray and Optical Sensors

[1]J. A. Nousek, [2]M. W. Bautz, [3]B. E. Burke,
[4]J. A. Gregory, [5]R. E. Griffiths, [6]R. L. Kraft,
[7]H. L. Kwok, [8]D. H. Lumb

To appear in the CRC Handbook on Measurement, Instrumentation and Sensors.

[1]Department of Astronomy and Astrophysics, 525 Davey Lab, Pennsylvania State University,University Park, PA 16802

[2]MS-37-415, Center for Space Research-MIT, 77 Massachusetts Avenue, Cambridge, MA 02139 Ctr. Space Research

[3]MS. LI-127, 244 Wood Street, P.O. Box 73, Lexington, MA 02137-9108

MIT [4]Lincoln Labs, ML-204A, 244 Wood Street, Lexington, MA 02137-9108

[5] Physics Department, Carnegie Mellon University, 5000 Forbes Avenue, Pittsburgh, PA 15213-3890

[6] Smithsonian Astrophysical Observatory, 60 Garden Street, MS-31, Harvard-Smithsonian Ctr. Astrophys. Cambridge, MA 02138

[7]Department of Electrical and Computer Engineering, University of Victoria, U. P.O. Box 3055, MS 8610, Victoria, BC, Canada V8W 3P6

[8]Astrophysics Division, ESTEC, Keplerlaan 1, Postbus 299, 2200 AG Noordwijk, The Netherlands

Charge-Coupled Devices as X-ray and Optical Sensors

J.A. Nousek, M.W. Bautz, B.E. Burke, J.A. Gregory, R.E. Griffiths, R.L. Kraft, H.L. Kwok, D.H. Lumb

1 Introduction

1.1 Use of CCDs for Precision Light Measurement

Charge-Coupled Devices (CCDs) have become the detector of choice for sensitive, highly precise measurement of light over the electromagnetic spectrum from the near-IR (shortward of 1.1 μm) to the X-ray band (up to 10 keV). Key advantages of CCDs over their predecessors (photographic emulsions and vacuum tube, electron beam readout devices such as Vidicons and SIT tubes) are high quantum efficiency, high linearity, large dynamic range, relatively uniform cosmetic response, low noise and intrinsically digital image capture.

CCDs were initially designed as serial data storage media (an electronic analogy to the magnetic Bubble Memory units) in which charge packets were injected into linked capacitors to store data, and read back by moving the packets back out of the device. When it was found that charge packets could be directly induced in the capacitors by exposing them to light, the CCD as light sensor was born.

Physically, the CCD operation consists of four critical stages. First, an incident light photon must be photoabsorbed in the sensitive portion of the CCD chip (called the depletion region). At optical and infrared wavelengths the absorption results in a single electron being promoted into the conduction band (leaving a hole behind), but at shorter wavelengths the photon has enough energy to make additional electrons via secondary ionizations by the photoelectron.

Second, the photon induced electrons must be collected, via an electric field within the silicon, into localized regions near the front surface of chip. The electric field is shaped by implanted dopants and by electric potentials applied to thin conducting strips (called gates) which prevent the electrons from diffusing away. The resulting charge distribution corresponds to an electronic analog of the light intensity pattern shone on the CCD. The granularity of this pattern is governed by the size of the potential wells, which are designed to be periodic. Each well is called a pixel, and corresponds to the minimum picture element detected by the CCD.

Third, after an exposure is completed the CCD charge pattern must be transfered out of the CCD. This is accomplished by modulating the potential applied to the CCD gates in such a way that no charge packets are mixed, but that each packet moves into the next pixel. The end pixel is transferred into a special pixel array called the serial register. Each movement of charge resulting from gate potential changes is called a clock cycle, and the serial register receives many clock cycles for each cycle of the full pixel array. The net result is a sequence of charge packets emerging from the serial register, each of which is directly proportional to the amount of light striking a particular location on the CCD.

Fourth, the emerging charges are converted into electrical signals by a charge sensitive pre-amplifier on the CCD chip. These signals are often digitized by electronics in the camera immediately outside the chip, but analog readouts which produce signals compatible with video standards are also used (the popular hand-held video cameras are examples of this). Research grade camera readouts are able to measure the

charge pulses with accuracies as good as one or two electrons rms, if the CCD and electronics are cooled.

Currently available CCDs carry out these steps so well that they are nearly the ideal detector for precision low light level applications, especially in astronomy. Such an ideal detector would have perfect quantum efficiency (i.e. convert every incident photon into detectable signal), have no noise, have unlimited dynamic range, have linearity in response to incident intensity and position, and have completely understandable characteristics. Modern CCDs succeed on all these counts.

CCDs have high quantum efficiency because photons interact via photo-absorption in the depletion layer which directly results in one or more electrons promoted into the conduction band of the silicon lattice, which are very efficiently collected by the CCD. The main obstacles to perfect quantum efficient are absorption of photons by the gate and insulator materials before they ever reach the depletion regions (or optically, by reflection off the front surfaces) or if the photon passes entirely through the depletion region without interacting (See Section 2.a).

There are many approaches to enhancing CCD quantum efficiency for various applications. In soft X-ray and ultraviolet wavelengths the gate and insulator layers on the front of the CCD absorb too much light. To solve this, CCDs are built with thin gates or thinned substrates and back-side illumination (See Section 3.c). CCDs are also coated with phosphor coatings which downconvert ultraviolet light to longer wavelengths where the gate transmission is higher (See Section 3.a).

At hard X-ray and infrared wavelengths too much light can pass through the depletion region without interacting at all. The depletion region is the part of the CCD pixel which is swept clean of free charges during the readout process. The depletion region gets deeper if higher purity silicon is used, and if higher voltages biases are applied during the readout.

Longward of 1.1 μm photons do not have sufficient energy to promote electrons into the silicon conduction band, so other materials, such as germanium or a compound semiconductor like InAs, InSb or HgCdTe must be used.

CCD noise results from four major factors: a) thermal background noise, b) charge transfer imperfections, c) charge-to-voltage amplification noise (capacitance noise), and d) cosmetic imperfections in the CCDs due to, for example, microscopic shorts in the insulating layers of the CCD. a) results from a 'dark current' of thermally excited electrons which accumulate in the pixels and can be eliminated by cooling the CCD (typically to -60 to -120 C). b) results from traps which hold electrons long enough to shift them into following charge packets identified with other pixels. c) is a fundamental limit related to the temperature and capacitance of the output mode (kTC), but can be kept intrinsically low because the capacitance of the amplifier can be made small, and signal processing techniques such as 'correlated double sampling' can reduce the noise to the equivalent of a few electrons (1-5 in state-of-the-art cameras). (See Section 2.d) b) and d) can be greatly reduced by improved manufacturing technique, especially scrupulous contamination control during the process.

CCD dynamic range is set by the maximum charge packet which can be stored in a pixel. Termed 'Full-Well Capacity', this is set by the depth of the potential well. When the Full-Well Capacity is exceeded the image of a point source 'blooms' as a result of charge leaking into surrounding pixels, and a trail of brighter pixels forms in the readout direction of the CCD due to charge incompletely transferring from pixel-to-pixel during a clock cycle. Modern CCDs have Full-Well Capacities in excess of 10^5 electrons, and can be designed even larger. (Note that larger Full-Well also requires larger output capacitance, so a trade-off is generally required between blooming and low noise.)

CCD linearity in intensity response and position response is very good, because the conduction band in the CCD has so many states that the very small injected photo-charge does not affect subsequent photon interactions. The position linearity results from the photo-lithography of the manufacturing process, which must be accurate to less than 1 μm. The primary limitation on linearity results from imperfect Charge

Transfer Efficiency (CTE) in the process of clocking charge packets from pixel to pixel. At readout rates below 100,000 pixels per second CTE imperfections have four causes. a) Design imperfections: errors in CCD design can leave potential minima which are incompletely drained during clocking. b) Process induced traps: random cosmetic defects presumably due to imperfections in manufacturing. c) Bulk traps: lattice defects or impurities which introduce local potential minima which temporarily capture electrons long enough to remove them from the original charge packet, but re-emit them later. d) Radiation induced traps: similar to c), but resulting from lattice defects caused by low energy protons. This damage is most commonly seen by spacecraft CCD cameras.

1.2 CCD Operation and Data Reduction

In order to achieve ultimate CCD performance for a given goal the CCD camera can be operated in special ways, and the post-camera data reduction can be optimized. Typical optical use of CCDs involves timed exposures, where the CCD pixels are exposed to light and the total charge integrated in pixels for a pre-selected time. At the conclusion of the integration a shutter closes and the CCD is read-out. As noise reduction limits the read-out to roughly 100 kpixels/second, a large CCD (2048x2048 pixels) readout can take many seconds to complete.

To avoid the deadtime associated with the closed shutter, some CCDs are made with framestore regions. The framestore is a pixel array equal to the integration region which is permanently blocked by a cover from any additional light. The pixels containing the charge pattern resulting from the integration are very rapidly clocked into the framestore region (typically requiring much less than one second) and then slowly clocked out into the readout region without moving the integration pixels.

Operationally CCD reduction requires calibration exposures. These include bias frames, which are read-outs with the same integration time but no light striking the CCD, and flat field frames, which have a uniform illumination over the CCD. The bias frames are subtracted from the data frames to set the zero-point corresponding to zero incident radiation. (Note that CCDs will accumulate charge due to thermal electrons and low level shorts in the gates, even if no light hits the CCD.) The flat field allows correction for pixel-to-pixel sensitivity variations. Proper flat fielding can remove variations of arbitrary amplitude and spatial scale.

The CCD dark current bias can be reduced by cooling the CCD, or by operating it in an inverted phase mode. In inverted phase operation the gate electrode is given a suitable negative bias which attracts hole carriers to the front surface of the CCD. These holes fill interface states at the Si-SiO_2 boundary between the conducting depletion region and the insulating layer under the gates. Suppression of these interface states dramatically lowers the dark current because the interface states are much more efficient at thermal electron promotion to the conduction band than the bulk material. Not all phases can be operated in inverted mode in a normal CCD because without the restraining potentials provided by gates held at positive voltage the pixel charge packets can intermingle. A special CCD called an MPP (Multi-Phase Pinned) device, has extra implant doping which isolates the pixels even with all three phases inverted, yielding dark current so low that integration times up to minutes become possible in room temperature MPP CCDs.

Other important uses of CCDs include cases where the CCD is continuously clocked, without any shutter. Suitable for high light level conditions, the effective integration time becomes the time to transfer a pixel charge across the source point spread function on the CCD. This allows sensitive timing of source intensity changes.

A similar technique is called drift scanning, where the rate of clocking of pixels equals the rate of motion of the target across the CCD. Such a condition is common in astronomy, where a fixed detector on the

Earth sees slow motion of stars in the field of view due to the Earth's rotation.

Drifts and instabilities in the camera electronics can be corrected by use of a technique called 'overclocking'. If the serial registers are clocked more times than there are physical pixels in the CCD, then the excess clocks will produce charge pulses corresponding to zero input light and zero dark current. The distribution of the overclock pulse is then a measure of the readnoise of the CCD chip-camera system, and the mean of the distribution sets the zero point of the energy to output voltage curve. Frequently CCD cameras subtract the mean of the overclock pixels from all output values in a row (called 'baseline restoration').

1.3 CCD Signal-to-Noise Ratios (S/N)

To see how these characteristics of the CCD relate to measurement it is instructive to study the S/N predicted for a given exposure time. In a single pixel illuminated by a source which contributes S_o counts (electrons) to the pixel, we also will see contributions from dark current (S_d) and background illumination (S_s; usually called the 'sky' in astronomical usages), all in units of counts/pixel/second. The source contribution (S_o) can be expanded into the intensity of light from the source, I; the quantum efficiency of the CCD, Q; and the integration time, t; to provide

$$S_o = I \times Q \times t \tag{1.1}$$

The camera readout contributes a randomly distributed, but fixed Gaussian noise with variance N_r.

The Signal-to-Noise (S/N) of a particular pixel is then:

$$S/N = I \times Q \times t/(I \times Q \times t + N_r^2 + S_d + S_s)^{1/2} \tag{1.2}$$

If the light from a source is distributed over a number of pixels, n, (as might arise from a star viewed through a telescope with a Point Spread Function (PSF) covering n pixels), then if the integral of S_o over the PSF is C_o, and the integral of S_s over the pixels is C_s, then

$$S/N = C_o^{1/2}/(1 + C_s/C_o + n + r^2/C_o)^{1/2} \tag{1.3}$$

Clearly, high Q and low r are desirable, and t should be chosen to make C_o greater than both C_s and r. It is worth noting that in most optical applications (except for extremely faint sources) it is the uncertainty in the 'flat fielding' (i.e. the corrections made for pixel-to-pixel sensitivity variations and background) that ultimately limits the achievable S/N.

2 CCD Structure and Charge Transport

2.1 CCD structure and its potential profile under bias

A CCD is a semiconductor device operating under the principle that charges can be temporarily stored and transported along a string or array of MOS capacitors. The basic storage unit is called a pixel and is made up of several MOS capacitors. In almost all CCDs charges are stored either directly at the oxide-semiconductor interface (surface-channel device), or deeper within an epitaxial layer (buried-channel device). Theoretically, a surface-channel CCD has a larger charge capacity, but it also is prone to noise arising from interface states at the boundary.

The CCD is operated by varying voltages applied to the surface electrodes. Typically the CCD is kept for a long period in an integration state, where photon induced electrons accumulate in the potential wells

under the CCD pixels. After the integration finishes the voltages are changed to transport the charge from one capacitor to the next. This sequence of moving charge packets by potential clocking is sometimes called 'bucket-brigade' charge transfer.

The storage unit of the CCD is the MOS capacitor and it is possible to deplete, invert or form a surface accumulation layer in the MOS capacitor by simply changing the surface potential. CCDs operate in the so-called 'deep depletion' mode when the surface layers are fully-depleted. For a buried-channel CCD with an n-type buried layer within a p-type epilayer, this would require the application of a positive bias to the surface electrodes. The equations governing the 1-dimensional calculations of the potential distribution in the MOS capacitor are [1]:

$$\begin{aligned} \frac{d^2\psi}{dx^2} &= 0 & -d < x < 0 \\ \frac{d^2\psi}{dx^2} &= -q \cdot \frac{N_D}{\epsilon_s} & 0 < x < t \\ \frac{d^2\psi}{dx^2} &= q \cdot \frac{N_A}{\epsilon_s} & t < x < x_p \end{aligned} \tag{1.4}$$

where ψ is the potential, N_A is the substrate acceptor density, N_D is the donor density in the epilayer, X_p is the depletion edge in the p-type substrate and ϵ_s is the semiconductor permittivity. Note also that d is the oxide thickness and the origin ($x = 0$) is located at the oxide-semiconductor boundary.

The boundary conditions will be:

$$\begin{array}{ll} \psi(x = -d) = V_G & \frac{d\psi}{dx}|_{x=t^-} = \frac{d\psi}{dx}|_{x=t^+} \\ \epsilon_o x \cdot \frac{d\psi}{dx}|_{0^-} = \epsilon_s \cdot \frac{d\psi}{dx}|_{0^+} & \psi(x = t^-) = \psi(x = t^+) \\ \psi(x = 0^-) = \psi(x = 0^+) & \psi(x = t + x_p) = 0 \end{array} \tag{1.5}$$

and the solutions are:

$$\begin{aligned} \psi &= V_G - E_{ox} \cdot (x + d) & -d < x < 0 \\ \psi &= \psi_{max} - q \cdot N_D \cdot (x - x_n)^2/(2\epsilon_s) & 0 < x < t \\ \psi &= q \cdot N_A \cdot (x - t - x_p)^2/(2\epsilon_s) & t < x < t + x_p \end{aligned} \tag{1.6}$$

where E_{ox} is the electric field in the oxide layer, V_G is the gate bias voltage and x_n is the position of the potential maximum.

Fig. 1 shows a typical potential profile across the MOS capacitor in a buried-channel CCD. Note the presence of a potential maximum, ψ_{max}, where the electrons will reside. It is given by:

$$\psi_{max} = \psi_J \cdot (1 + N_A/N_D) \tag{1.7}$$

where $\psi_J = q \cdot N_A \cdot x_p^2/(2\epsilon_s)$. Since x_p increases linearly with N_D, the potential maximum ψ_{max} and hence the charge storage capability also increases for a heavily doped epilayer. The derivation of the potential profile in a surface-channel CCD will be similar, but with d set to zero.

2.2 Charge Transport

Charge transport in a CCD refers to the transfer of charges along the MOS capacitors (i.e. from one pixel to the next). There are several clocking schemes used, generally divided according to how many external voltage regions are applied per pixel, ranging from one (uni-phase) to four-phase.

Computation of charge transport in a CCD requires solving the 2-dimensional Poisson equation with appropriate boundary conditions to obtain the potential distribution within the pixel for each separate phase within the clocking cycle. Numerical techniques using finite-difference or finite-element methods have been used. For charge transfer in an n-type epilayer, the electron flux, F(x), is given by:

$$F(x) = n_s(x,t) \cdot v(E(x)) - D(E(x)) \cdot (n_s(x + \Delta x, t) - n_s(x,t))/\Delta x \tag{1.8}$$

where $N_s(x,t)$ is the electron density, E(x) is the electric field in the x-direction, v(E(x)) is the field-dependent velocity and D(E(x)) is the electron diffusivity. Fig. 2 shows the time evolution of charges along a CCD. Some 'smoothing' of the output charge profile is often observed and for high-speed devices velocity saturation will be important. Computations of charge transfer is sometimes carried out by using a equivalent circuit model for the CCD in a SPICE-type simulator. It has been shown to offer both faster computation time and the ability to include external support circuits into the model.

Charge transfer efficiency, η, in the key figure-of-merit in a CCD, at least comparable to quantum efficiency. A common technique to determine η is to measure the amplitude response of the CCD using a network analyzer. η is then related to the amplitude response of the output, G_V through the following relationship:

$$G_V = \exp\{-N_T \cdot (1-\eta) \cdot [1-\cos(2\pi f/f_c)]\} \tag{1.9}$$

where N_T is the number of transfers, f is the signal frequency and f_c is the clock frequency. For the relatively mature Si CCD technology charge transfer efficiency of 0.99999 can be easily achieved. Note, however, that this analysis applies to sinusoid illuminated scenes and test signals, but does not apply to delta function injections of charge which are infrequently transferred, as applies to the X-ray photon-counting case.

2.3 Input and Output Structures

The input structure of the CCD usually consists of a p-n junction and two or more input gates as shown in Fig. 3. Initially, when the input voltage, V_{id} is pulsed low, charges will flow through the input (electrode) into the potential well created under the input gates G_1 and G_2. When V_{id} returns to its equilibrium value, charges will be withdrawn except those residing in the potential well formed by the potential difference between G_1 and G_2. Charge injection is now complete and a drop in the potential Φ_1 at the transfer gate will allow charges to enter into the first CCD pixel. The input charge, Q_{in}, is approximately given by:

$$Q_{in} = C_{ox} \cdot (V_{G1} - V_{G2}) \tag{1.10}$$

where C_{ox} is the oxide capacitance and V_{G1} and V_{G2} is the voltage difference between G1 and G2. In CCD sensors and detectors signal input normally relies on the incident photons liberating charge within the depletion region (after traversing either the front gates [front-illuminated] or the back surface [back-illuminated]). Charges so created will be collected in the potential wells formed by the clock voltages.

Normally the output structure of the CCD consists of a reset switch and a floating diffusion (FD) or floating gate (FG) amplifier. (See Section 3.3). These are shown in Fig. 4. During sampling, the output charge flows into the floating node and a voltage is developed across the output capacitance which is a combination of the depletion capacitance of the floating node and the input gate capacitance of the source follower. In general, the voltage output, V_{sig}, can be expressed as:

$$V_{sig} = Q_{inj} \cdot A_V / C_{fd} \tag{1.11}$$

where Q_{inj} is the injected charge, A_V is the small-signal voltage gain of the output amplifier and C_{fd} is the capacitance between the floating node and ground. Since both A_V and C_{fd} are sensitive to the output charge and temperature, this type of output structure is not generally linear. Improvements in the output structure can be achieved by using either a floating gate amplifier or Miller feedback at the output to reduce parasitic capacitances.

2.4 Noise in CCDs

Noise in CCDs will degrade the S/N ratio (Sec. 1.3). The following are important noise sources in CCDs:

1) Thermal noise, or dark current, is due to thermally excited electrons which accumulate in the pixels during the integration. In applications where the clocking time is short compared to the integration time the equivalent noise election, n_{th}, is given by:

$$n_{th} = \sqrt{J_d \cdot A_E \cdot t_{int}} \tag{1.12}$$

where J_d is the leakage current density, A_E is the area of the transport electrode, and t_{int} is the integration time. A lowering of the operating temperature will normally reduce the leakage current density and hence the equivalent noise electron.

2) Bulk traps are the dominant noise sources for buried-channel CCDs and the equivalent noise electron from this source is:

$$n_{trap} = \sqrt{N_t \cdot V_{sig} \cdot Nt \cdot e^{-T_t/\tau_e}[1 - e^{-T_t/\tau_e}]} \tag{1.13}$$

where V_{sig} is the volume of the charge packet under the transfer electrode, N_t is the density of the bulk trap states, T_t is the transfer time and τ_e is the electron emission time constant. It can be observed that the equivalent noise electron increases as the size of the charge packet increases, an indication that bulk traps do not generally affect the S/N ratio in CCDs. In X-ray photon counting applications some effects of bulk trapping noise have been seen.

3) Both the input and output of a CCD involve charge storage across capacitors which will be affected by fluctuations in the circuit. The equivalent noise electron for this process is:

$$n_{inp} = \sqrt{kT \cdot C_{inp}} \quad n_{out} = \sqrt{kT \cdot C_{out}} \tag{1.14}$$

where kT is the thermal voltage and C_{inp} and C_{out} are the input and output capacitances. A special signal processing technique known as 'correlated double sampling' can be used to reduce this kTC noise at the CCD output.

1/f noise is also present in the output amplifier and is only significant at low frequency. Methods to reduce 1/f noise include multiple sampling using distributed floating-gate amplifiers (DFGA) [2] and noise cancelation techniques using alternate gain inversion (AGI) [7].

4) The maximum S/N ratio of a CCD is limited by the maximum amount of charge which can be stored in a pixel divided by the equivalent noise electron. Expressed in decibels it is:

$$S/N = 20\log(Q_{max}/Q_{noise}) \tag{1.15}$$

The maximum charge is:

$$Q_{max} = C_e \cdot \psi_{BH} \tag{1.16}$$

where C_e is the depletion capacitance associated with the electrode, and ψ_{BH} is the depth of the potential well.

2.5 Power Dissipation in CCDs

Power dissipation in a CCD is primarily linked to the charging and discharging of the gate capacitances. This power is mainly consumed by the clock driver and is given by:

$$P_{clock} = C_c \cdot V^2 \cdot f_c \tag{1.17}$$

where C_c is the clock line capacitance associated with the electrodes, V is the clock voltage and F_c is the clock frequency. For $f_c = 100$ MHz and $V = 5$ V, this would imply $P_{clock} = 50\mu$W/pixel.

In addition to P_{clock}, the on-chip power dissipation/pixel is approximately given by:

$$P_{CCD} \approx nq(f_c L)^2/\mu_e + 2nqf_c(\psi_{BH} - nq/(2C_e)) \tag{1.18}$$

where n is the number of electrons in a pixel, L is the pixel length and μ_e is the electron mobility. The overall power dissipation in a CCD is therefore the sum of P_{clock} and P_{CCD}.

3 Applications of CCDs to Light Sensing

3.1 Optical Imaging and Spectroscopy

The many fine properties of CCDs have made them the detector of choice for the recording and readout of images at both high and low light levels. The applications include (i) reconnaissance, both civilian and defensive, (ii) scene and personnel monitoring, (iii) robotics and (iv) astronomy. In astronomy, CCD cameras have found their way into almost all observatories in the world, both for direct readout of images and as the readout cameras for spectrographs.

Perhaps the most exacting application of CCD's has been to astronomy, a discipline in which the characteristics of the CCD need to be pushed to their limits in order to gain the optimum performance. As well as the attempt to optimize this performance in order to gain as much science as possible from the images, it has also been crucial to calibrate the devices as well as possible and to fully understand their behavior. In this sense, astronomy has been the "driver" for the scientific development of CCDs. Large-scale commercial applications, such as video recorders, monitoring cameras, etc. have driven the need for improved manufacturing yield, blemish-free operation, uniformity in performance, and reliability.

In order to illustrate the importance of CCDs to exacting scientific requirements, this section will again focus largely on the applications to astronomy.

The early demonstration of the performance of a commercial CCD at the focus of a telescope quickly led to the realization of their potential for both space and ground-based astronomical cameras and instruments. Fortunately, this development in the early 1970's was just in time for the first major optical observatory in earth orbit, the Hubble Space Telescope (HST). Perhaps the most spectacular application of CCDs to visible light imaging has been within the cameras on board this telescope, i.e. the Wide Field and Planetary Cameras built at the Jet Propulsion Laboratory. The CCDs in these cameras consisted of 800x800 pixel arrays, with each pixel of size 25 microns. The first version of this camera contained eight thinned, back-illuminated devices which were more or less fully depleted. An accumulation layer at the back surface was achieved by flooding the devices with UV light from a lamp internal to the instrument. This accumulation layer allowed the collection of charge resulting from the photoelectric absorption of blue light, and accelerated the charge to the frontside potential wells. Furthermore, the devices were coated in a down-converting coronene phosphor which converted UV light into the yellow-green wavelength band, thus allowing a 20UV. These devices thus had relatively high quantum efficiency from the UV through to about 1 micron, vitally important for an instrument collecting photons from galaxies billions of light years away in the universe. As well as their high quantum efficiency, these devices had high charge transfer efficiency and relatively low readout noise at the time of their development. All of these characteristics have since been superseded - at first by an improved version of the camera installed in the Space Telescope in late 1993, and then in the Advanced Camera for Surveys, to be installed in 1999. These later instruments had larger format, higher quantum efficiency and lower readout noise. During the 1980's, devices were developed with these large formats and with readout noise levels approaching one electron rms, as described in section 3.3.

Starting with modest arrays of size of order a few hundred pixels in the 1970's, the devices which became available in the 1990's were as large as 4096 pixels square. As well as in space, these devices have been employed at the prime foci of the world's largest telescopes to give images covering more than 10 arc minutes on a side while still sampling the atmospheric-limited resolution (arcsecond or sub-arcsecond) adequately. Such devices, when exposed to the sky for up to an hour through a broad-band filter, can produce images with tens of thousands of objects for statistical studies in astronomy.

Typical pixel readout rates for astronomical cameras are of the order of 50kHz, taking tens of seconds for a full readout. Integration times for astronomical CCD cameras can vary from fractions of a second to tens of minutes or even times in excess of an hour, usually limited by the background noise induced by cosmic ray particles and their secondaries. These cosmic ray "events" can be removed by taking at least two frames of data and cross-comparing them. This is important even on the ground, where the radioactive background and muon-induced events total about one per sq. cm per minute; but the cosmic-ray background in space is about one per sq. cm per second, so that camera exposures are rarely longer than ten or twenty minutes. Sophisticated computer algorithms have been developed in order to remove the effects of this background radiation.

Of special importance to applications in space research is the packaging of the devices. Contamination of the cold CCD surface by as much as a monolayer of a heavy molecule will effectively render the CCD useless in the vacuum UV, for example. Careful attention has therefore to be paid to the local instrument environment. The CCDs on the Space Telescope were in hermetically sealed packages, and the contamination problem was transferred to the lenses covering the CCD packages. In order to achieve optimum performance, the overall camera has to be designed to satisfy the exacting requirements of the CCD, from the point of view of thermal control and stability, absence of electronic interference, and rigorous attention to the elimination of water or heavy molecule contamination. For space application, it may also be advantageous to surround the CCD package with a cosmic-ray shield, such as the 1 cm of tantalum used in the CCD cameras on HST and the Galileo mission to Jupiter. Such radiation shields have to be designed with caution, lest they introduce more secondary particles and induced radioactivity than the primary protons which they stop (section 3.3).

Finally, much effort is put into the processing of astronomical CCD data [24]. Special techniques have been developed to calibrate the pixel-to-pixel nonuniformity in quantum efficiency (a function of wavelength), both on large and small scales. With some effort, this nonuniformity can be calibrated to levels below 1%. Although it may be easy to expose the CCD to a diffuse source such that there are at least 10,000 electrons per pixel, the corresponding "flat-field" calibration accuracy may be compromised at low light levels. For astronomical applications, especially in space, most of the pixels may receive only tens of electrons or fewer during an exposure. Low-level traps (including those caused by cosmic radiation) will then manifest themselves in the form of charge-transfer inefficiencies over localized areas or columns. It may be important to calibrate the CCD at the same exposure levels as those typically encountered during the science observation. One way of effecting this is to use hundreds or thousands of frames of data taken in different parts of the sky, and rejecting the astronomical objects in them. These "sky frames" can then be used to produce a "super sky-flat" which is the average of the individual frames of data.

3.2 X-ray Imaging Spectroscopy

Scientific applications such as astronomy have been responsible for driving improvements in CCD technology. In the X-ray domain, for example, CCDs are starting to be employed for medical radiography, where the digital imaging capability and high sensitivity allows for lower patient doses and on-line image processing. As high resolution readout detectors of dispersive X-ray spectrometers, CCDs are becoming widely

used in the new generation of high brilliance synchrotron beamlines. As spectrometers, they are also being considered in some applications as replacement for Si(Li) diodes, where the higher operating temperatures and improved resolution and efficiency down to X-ray energies below 1 keV leads to applications of interest to biological science and technology.

In contrast with optical imaging applications with many photons per charge packet, to measure X-ray spectral information directly with a CCD, single photons per pixel per image frame are required. To use the CCD as a non-dispersive X-ray spectrometer requires that the correspondence between the magnitude of the electron charge packet generated initially by the X-ray photon, and the signal measured at the CCD output must be maintained. This places a very stringent requirement on the efficiency of charge transfer. However, even before the process of charge transfer is initiated, the physics of the charge collection may also degrade the energy measurement process.

The absorption process for a photon of energy E begins with the ejection of a photoelectron, of energy $E - E_B$, where E_B is the binding energy of the appropriate silicon atom electron shell. The range of the photoelectron may be only a fraction of a micron. In a few percent of cases a silicon K shell fluorescence photon may be emitted, and this has a range of about 10μm, so that there is a finite probability of the event energy splitting into more than one pixel.

Eventually a proportion of the energy is converted to free electrons, the rest into phonons. If this free electron charge packet is created in the depletion layer of the CCD, it is promptly drifted under the influence of the electric field to the buried channel collection site. During this drift time (t_d), the charge may laterally diffuse within a radius $\sim \sqrt{2Dt_d}$ where D is the diffusion constant. Except for the charge clouds originating deep in the depletion layer, this radius is small compared with the typical pixel size. If the charge is generated in a field-free layer *outside* the depleted volume, it will radially diffuse until a fraction recombines or reaches the depletion layer. The latter fraction then starts to drift with the same additional lateral drift as the depletion layer charge packets.

The pixel boundaries are loosely defined by the asymmetric fields created by electrode biasing schemes and surface channel stop implants, and not hard physical boundaries. Hence any lateral spreading processes may allow some splitting of the initial charge packet between pixels. Furthermore charge *loss* may be experienced either by the partial recombination of events when liberated deep below the depletion layer, or if the fraction of split charge is too low to be recognized against the device noise level.

In astronomical applications, in space-borne observatories, there is a continuous low level background of charged particles. Rather than liberating point-like charge clouds, they liberate a population of signal electrons along their tracks throughout the silicon. They may be easily discriminated against X-rays if these tracks are highly skewed with respect to the silicon surface and cross many pixels. Also, if the track is long enough, the magnitude of total charge cloud generated may be large compared with the typical X-ray charge packet.

These features impose a requirement to perform event recognition and analysis. To perform this on-ground would require transmission of all pixel data, including empty pixels, which for mega-pixel CCD frames generated on second time scales is quite infeasible. Performing this recognition on-board first requires a comparison against some lower threshold. Selection of this level is critical - too high and some split charge may be neglected with a consequent degradation of energy resolution. Too low a threshold, and many spurious events will be counted. If there is a drift or change in the zero energy signal upon which this threshold is applied, the energy scale may be mis-registered, and/or the relative fraction of events selected at different X-ray energies may be unknowingly altered. Simulations show that for the potential energy resolution of CCDs, spectral analysis of cosmic plasmas will demand a calibration of relative detection efficiency versus energy to $\sim$3%. If the threshold value is set at about 4σ times the readout noise, this calibration may be degraded by as little as a single digital bit of a commonly used 12-bit ADC in the CCD

readout electronics. Thus the real-time digital processing of events is required to be fast and complex.

A further complication of the event splitting is that to avoid pile-up in CCD frames, the probability of having multiple events per pixel is made more stringent by requiring surrounding pixels to have no signal, and allow this recognition process. Typically an event rate of 1 photon per 200 pixels per CCD frame is therefore imposed, but this places a rather low limit on attainable count rate performance. Especially with high resolution focusing optics of observatories such as AXAF[5], this can be much lower than for many previous experiments. If the core of the point spread function of the mirror is not to be degraded by this effect, then special readout formats that reduce the imaged area, in order to accelerate frame readout times, must be employed.

3.3 Future Improvements to CCDs

Backside CCDs

The useful spectral range of conventional CCD detectors, though quite broad, is limited in part by the presence of the polysilicon gates on the front surface. As is illustrated in Figure 5, photons with wavelengths in the range ($\sim$30 Å $< \lambda <$ $\sim$4000 Å) have attenuation lengths in silicon less than the typical thickness of the gate structure ($\sim$ 0.4μm). Photons in this spectral range are therefore absorbed before they can enter the photosensitive volume of the detector. For conventional CCDs the detection efficiency is no more than a few per cent in this band. If the gates can be made thinner by an order of magnitude, or avoided altogether, then the detection efficiency can be improved dramatically in both the very soft X-ray and the UV. Efforts following the former approach are described below. The latter strategy, which requires illumination of the back surface of the CCD (that is, the surface opposite the gates) is discussed here.

There are a number of techniques that can be used to produce back-illuminated devices [10,11,12], but they must all deal with two constraints: lateral diffusion of the photoelectrons before they are captured in the buried channel of a specific pixel and the tendency for photoelectrons to recombine at the back surface of the Si.

The lateral diffusion of electrons can lead to a loss of resolution of the CCD since they may cross the boundary between one pixel and another, leading to an erroneous assignment of the origin of the photon that created the electron. This problem is minimized by thinning the back illuminated CCD to thicknesses that are on the order of the depletion depth of the Si, so the least drift occurs before the electron is captured in the potential well of the buried channel. This thinning is accomplished by a combination of methods including mechanical grinding and polishing and wet etching. Handling of back illuminated CCDs after thinning, however, is a problem since the remaining Si is between 10 and 100 μm thick, and is not strong enough to support rough handling, or even the intrinsic stresses arising from the initial fabrication of the CCD. To circumvent this problem, rim thinning or frame thinning can be used; in the first case, a rim several mm wide around the circumference of the wafer is protected during the thinning process, while in the latter, a region one or two mm wide around each device is protected.

Lateral diffusion can also be reduced by imposing an electric field through the thickness of the thinned membrane, but if this is done by imposing an electrode on the back surface, then the device will have a reduced QE (quantum efficiency) due to absorption in this layer. The presence of a depletion region in the CCD will also give rise to an electric field, which reduces the lateral diffusion of electrons, but if the desired depletion region is on the order of tens of μm, in order to image high energy X-rays or IR photons, then the induced field will be small, due to the low doping levels in the silicon and Gauss' law.

Although the lateral spread of photoelectrons is a problem, the loss of carriers to recombination at the back surface presents a greater technical difficulty. The recombination velocity can be minimized by introducing a strong electric field at the back surface and by passivating this surface. There are several

methods employed to generate this electric field: one is by implanting carriers (p-type for the case where photoelectrons are to be captured) and annealing the sample to activate these carriers [11], a second is to deposit a thin layer of metal with the appropriate work function difference (typically Pt or another transition metal) [10], while a third method is to grow a heavily doped epitaxial layer on the back surface [13]. In the implant method, strong electric fields can be generated and the annealing process can help to passivate the back surface, but high temperature annealing of the wafer can present a problem if metalization is present, unless excimer laser annealing is employed [14]. Deposition of a thin metallic layer can lead to long term instability of QE and does not appear to yield the highest QEs. Deposition of an epitaxial layer relies on the use of sophisticated equipment and surface cleaning methods.

In addition to introducing an electric field on the back surface, it is necessary to electrically passivate that surface to lower the electron recombination velocity. Again, there are several approaches; the flash gate technique is probably the simplest, relying on inserting the sample in a steam atmosphere, but it is not stable over time [10]. Another method is to grow a high quality oxide on the back surface [11], but this requires the use of high temperatures, which could melt metalizations and allow any dopant layer to diffuse too deeply into the silicon.

Although the aim of the backside treatment process is always to maximize the fraction of charge collected from the vicinity of the back surface, there are subtle differences in requirements that depend on the application. In the UV (1000 Å $< \lambda <$ 4000 Å), the extremely small attenuation lengths (see figure 5) place a premium on non-negligible ($\gtrsim$ 50%) charge collection efficiency very close to the back surface. Therefore in UV sensors the field in the immediate vicinity of the the back surface is extremely important. Moreover, the real part of the index of refraction of silicon is quite high in the UV and optical bands, and Fresnel reflections limit the external detection efficiency that can be achieved. Thus significant improvements in the UV response of back-illuminated CCDs have been obtained via the application of antireflection coatings as a part of the backside treatment process [12].

In the very soft X-ray range (20 Å $< \lambda <$ 100 Å), the attenuation length can be larger by a factor of 10 than in the UV. Moreover, the primary photoelectron energy is large enough in this case that its range is comparable to the attenuation length [15], so the physics of the secondary ionization process becomes important. Thus in the very soft X-ray regime, it is the average properties of the device over scales of a few thousand Ångstroms that determine performance. However, for spectroscopic applications, the theoretical limit of device performance cannot be reached unless the charge collection efficiency substantially exceeds $\sim$ 90%. Thus in the soft X-ray one requires very high collection efficiency over a relatively large volume in the vicinity of the back surface.

Any back side fabrication techniques will probably require compromises to be made, but it is possible to achieve very high external QE in the UV, as shown in the accompanying figure 6, and in the soft X-ray region where 77% QE has been achieved at 277 eV [16]. Further improvements are necessary to achieve good results in the vacuum UV and theoretical limits for energy resolution in the soft X-ray. These improvements are possible, but will probably depend on the continued development of sophisticated processing tools.

Thinned Gate CCDs

Recently a new type of CCD was developed that was optimized for spectroscopy below 1 keV. This detector, called a thin gate CCD (or TGCCD), contained two novel features; floating gate output amplifiers (FGAs or 'Skippers') and thin gates (electrodes) [2]. The goal was to develop a detector that had Fano limited energy resolution with non-negligible QE over the 200 eV to 1000 eV bandpass. In this section, we will briefly describe this detector and compare it with more conventional CCDs.

Most conventional CCDs use a floating diffusion amplifier (FDA) to read out the signal charge. The readnoise of the FDA has improved from several hundred electrons (rms) in the 1970's to less than 3

electrons in the last few years [3]. The energy resolution of CCDs over the entire soft X-ray bandpass is now limited by factors other than readnoise. It is desirable to push the readnoise down from a few electrons to a fraction of an electron because it allows photons of lower energy to be detected in single photon counting mode.

One method to further reduce the readnoise is to read out the same charge packet multiple times. The signal charge is destroyed when read out through an FDA. In the FGA, however, an insulating gate is placed between the charge transfer channel and the output node. Gates around the output node are used to read out and withdraw the signal charge multiple times. The readnoise is then reduced by the square root of the number of read outs. Effective readnoises of less than 1 electron have been demonstrated using the FGA [2,4], and photons of energy 66 eV (Al L_α) have been detected using the TGCCD. If the readnoise could be pushed to a fraction of an electron, it would be possible to detect optical photons in single photon mode.

Lower Readnoise

The other novel feature of the TGCCD is its electrode structure designed to maximize soft X-ray QE. Most conventional front side illuminated CCDs have several thousand angstroms of SiO_2/Si_3N_4 insulator and Si electrode on the surface. These layers strongly limit the quantum efficiency of the device below 1 keV, but Fano-limited energy resolution is routinely achieved. The conventional solution to increase the low energy QE has been to etch away the back surface of the device and illuminate it from behind (a back side illuminated CCD). The difficulty with this technique is that the energy resolution is seriously degraded due to charge diffusion and poor charge collection.

The thin gate CCD is a front side illuminated device with a unique gate structure that gives reasonable soft X-ray QE (0.20 at 277 eV), while retaining the good energy resolution of front side illumination. The detector is a three phase CCD. The first two phases (comprising only 1/3 of the active area of the device) are covered with 4000 Å of polysilicon (or just poly) in the usual way. A third layer of poly is deposited on top of the first two which acts as a bus for a fourth (400 Å thick) layer of poly that defines the third clock phase. Two thirds of the active area of the detector is therefore covered with only the insulator (1000 Å of SiO_2 and Si_3N_4) and this fourth layer of poly. The measured energy resolution of this device is 34 eV at C K_α (277 eV). This is approximately a factor of 3 better than the best energy resolution obtained with the ACIS back side illuminated CCDs [5]. Simulations show that an astrophysical spectrum obtained with TGCCD contains as much or more information than one obtained with a back side illuminated CCD [6].

Radiation Damage

CCDs are often used in environments in which they are subject to ionizing radiation, and this radiation can degrade their performance. In particular, radiation damage plays an important role in the performance of most space-borne detectors. The Van Allen belts contain protons and electrons with energies of tens of MeV. These particles can produce damage by several mechanisms. Protons can generate vacancy-interstitial pairs in the Si lattice, which diffuse freely, even at cryogenic temperatures, and it is possible for the vacancy to form a complex with P atoms in the n-Si buried channel which traps electrons. The trap reduces CTE by preventing signal electrons from leaving the pixel during the clocking cycle. Electrons, too, can produce vacancies (though with much lower cross-section than the protons), but they can also create dangling bonds at the SiO_2-Si interface above the buried channel, leading to a shift in operating voltage in the CCD and contributing to noise.

The P-V complexes remove electrons from a charge packet in the conduction band of silicon. In the worst case limit, when the illumination levels are so low that each charge packet transferred encounters

each trap in its empty trap state, the degradation of CTE is approximately 5×10^{-7} rad^{-1} (radiation doses are expressed here in total ionizing rads in Si, though it should be noted that the fraction of proton energy which goes into production of vacancy-interstitial pairs, the non-ionizing energy loss, is about 1/2000 of the total ionizing dose [17].) This degradation is significant: if the device is subjected to 1000 rad yr^{-1} and there are 1000 transfers necessary to clock out the charge, then 40% of the charge packet would be lost due to proton induced defects. At higher illumination levels the traps greatly complicate the device response, particularly in single-photon counting applications. In this case, for example, the spectral response of the CCD becomes a function of the spatial distribution of the incident radiation.

This loss of CTE can be circumvented in several ways, including the use of increased shielding, a fat zero, annealing out the damage, implanting a narrow trough along the direction of transfer in the buried channel, or operating the device at different (generally lower) temperature.

Relatively thick shielding, up to the equivalent 4-5 cm of aluminum, can provide significant attenuation (factors of several) of proton dose encountered in the radiation belts [18]. A fat zero is a uniform charge added to all the pixels of the CCD, usually induced by flooding the CCD with a low light level. Although a fat zero can reduce the CTE loss by filling the traps so they cannot be occupied by electrons from the charge packet of interest, they also add to the noise of the system. The P-V complex will dissociate at temperatures around 135 C [19], but the annealing is incomplete and may interfere with other requirements or constraints of the satellite mission. Using photolithography, a narrow trough or notch can be included in the buried channel parallel to the direction of transfer during fabrication, so charge packets are kept constrained and are less likely to interact with traps generated randomly across the buried channel [20]. It is not difficult to introduce a channel that is approximately 2 μm wide and can handle a charge packet of tens of thousands of electrons; this can decrease the CTE loss to 7×10^{-8} rad^{-1} or less. Reducing the operating temperature slows the kinetics of trap emptying [21], so a single electron can be lost from the charge packet and fill the trap for the integration time of the frame. The effectiveness of this process depends on the clock speed and integration time, as well as the ability to operate the CCD at temperatures that approach -150C, but CTE loss can be as low as 10^{-8} rad^{-1} if troughs are included with low temperature operation. Cosmic rays and electrons can also cause damage by displacing Si atoms from the lattice, but the flux of cosmic rays is much lower than protons in low earth orbits and the electrons are much less effective in creating a vacancy. The approaches to hardening against proton damage will also be effective with these latter two particles.

The major effect of electrons on CCDs is to shift the flatband voltage of the CCDs and MOSFETs, but for doses around 1000 rads this change is on the order of 10 mV. If further hardening of the gate oxide is desired, it can be accomplished using established methods [22]. The passage of electrons and other energetic charged particles through a device also creates free carriers which constitute an interfering signal. One electron-hole pair is created for each 3.65 eV absorbed in the Si, and charged particles can deposit charge packets of up to a full-well level and more, depending on the species, energy, and the active depth of the device. In astronomy, such events are an annoyance, even in terrestrial observatories, and are removed by comparing images of the same scene. In some applications, such as x-ray spectroscopy, these events are more serious because they can masquerade as desired signals unless careful analysis of the data is performed to exclude them. On the other hand, this sensitivity to charged particles can actually be used to advantage. The known conversion between particle energy deposition and liberated charge means that CCDs can be used as spectroscopic detectors, and such an application has been proposed for inertial-confinement fusion diagnostics [23].

Radiation hardening of CCDs has made rapid progress in the last few years, allowing devices to have much longer lives for scientific applications. Fabrication and operational changes have increased the hardness to displacement damage and the process requirements of high quality ICs have led to a gate dielectric that is

quite robust to ionizing radiation.

4 References

[1] C.K. Kim, "The Physics of Charge-Coupled Devices", in M.J. Howes and D.V. Morgan, Eds., *Charge-Coupled Devices and Systems*, Wiley, New York (1979).

[2] R.P. Kraft, D.N. Burrows, G.P. Garmire, J.A. Nousek, J.R. Janesick, and P.N. Vu, Nucl. Instr. and Meth. **A361**: 372, 1995.

[3] D.N. Burrows, G.D. Berthiaume, M.A. Catalano, G.P. Garmire, C. Larkin, F. Marks, J.A. Nousek, and G.M. Weaver, EUV, X-ray, and Gamma-Ray Instrumentation for Astronomy and Atomic Physics, eds. C.J. Hailey and O.H.W. Siegmund, Proc. SPIE **1159**: 92, 1989.

[4] C.E. Chandler, R.A. Bredthauer, J.R. Janesick, J.A. Westphal, and J.E. Gunn, SPIE Symp. on Electronic Imaging, Proc. SPIE **1242**: 238, 1990.

[5] R.P. Kraft, D.N. Burrows, G.P. Garmire, J.A. Nousek, Ap.J.Lett. **466**: L51-L54, 1996.

[6] M.C. Weisskopf, S.L. O'Dell, R.F. Elsner, and L.P. Van Speybroeck, Proc. SPIE **2515**: 312, 1995.

[7] Y. Matsunaga and S. Ohsawa, IEEE JSSC V-SC26 **12**: 1902, 1991.

[8] D.F. Edwards, *Handbook of Optical Constants of Solids*, E.P. Palik ed., Academic Press, New York, 1985, p.547.

[9] B.L. Henke, P. Lee, T.J. Tanaka, R.L. Shimabukuro, and B.K. Fujikawa, Low Energy X-Ray Diagnostics, D.T. Attwood, B.L. Henke eds., AIP Conf. Proc. No. 75, American Institute of Physics, New York, 1981, p. 340.

[10] J.R. Janesick, D. Campbell, T. Elliott, and T. Daud, Opt.Eng. **26**: 852, 1987.

[11] J.A. Gregory, B.E. Burke, A.H. Loomis, and H.R. Clark, Solid State Research Report, Lincoln Laboratory, MIT, 1993:1, p. 53.

[12] M.P. Lesser, Inst. in Astronomy VIII, Proc. SPIE **2198**: 782 1994.

[13] M.E. Hoenk, P.J. Grunthaner, F.J. Grunthaner, R.W. Terhune, M. Fattahi, and H.-F. Tseng, Appl.Phys.Letts. **61**: 1084, 1992.

[14] C.M. Huang, B.E. Burke, B.B. Kosicki, R.W. Mountain, P.J. Daniels, D.C. Harrison, G.A. Lincoln, N. Usiak, M. A. Kaplan, and A.R. Forte, Proc. of the Int. Symp. on VLSI Technology, Systems, and Applications, IEEE, New York, 1989, p. 98.

[15] F. Scholze and G. Ulm, Nucl. Instr. and Meth. **A299**: 354, 1990.

[16] G.Y. Prighozin, submitted to IEEE Nuclear Sci. Symp., Nov. 1996, to be published in IEEE Trans. Nucl. Sci.

[17] M.J. Cantella, B.E. Burke, J.A. Gregory, D.C. Harrison, E.D. Savoye, and B.-Y. Tsaur, Infrared Focal Plane Arrays IIIA, J. A. Jamieson ed., Ballistic Missile Defense Organization, Washington, 1994, p. 10-1.

[18] K.C. Gendreau, M.W. Bautz, and G.R. Ricker, Nucl. Inst. and Meth. **A335**: 318, 1993.

[19] M. Hirata, H. Saito, and J. Crawford, J. Appl. Phys. **38**: 2433, 1967.

[20] T.S. Villani, W.F. Kosonocky, F.S. Shallcross, J.V. Groppe, G.M. Merais, J.T. O'Neill III, and B.J. Esposito, Proc. SPIE **1107**: 9, 1989.

[21] K.C. Gendreau, G.Y. Prigozhin, R.K. Huang, M.W. Bautz, IEEE Trans. Electron Dev. **42**: 1912, 1995.

[22] P.V. Dressendorfer, Ionizing Radiation Effects in MOS Devices and Circuits, T. P. Ma and P. V. Dressendorfer eds., John Wiley, New York, 1989, p. 333.

[23] B.E. Burke, R.D. Petrasso, C.-K. Li, T.C. Hotaling, to be pub. in Rev. Sci. Inst., Jan. 1997.

[24] G.H. Jacoby, ed. "CCDs in Astronomy", ASP Conference Series, Volume 8, 1990.

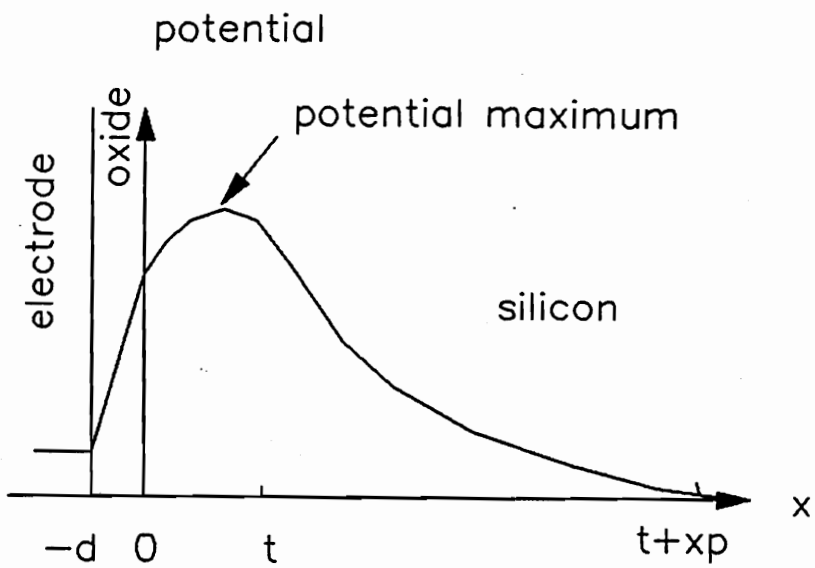

FIGURE 1. Potential profile across MOS capacitor.

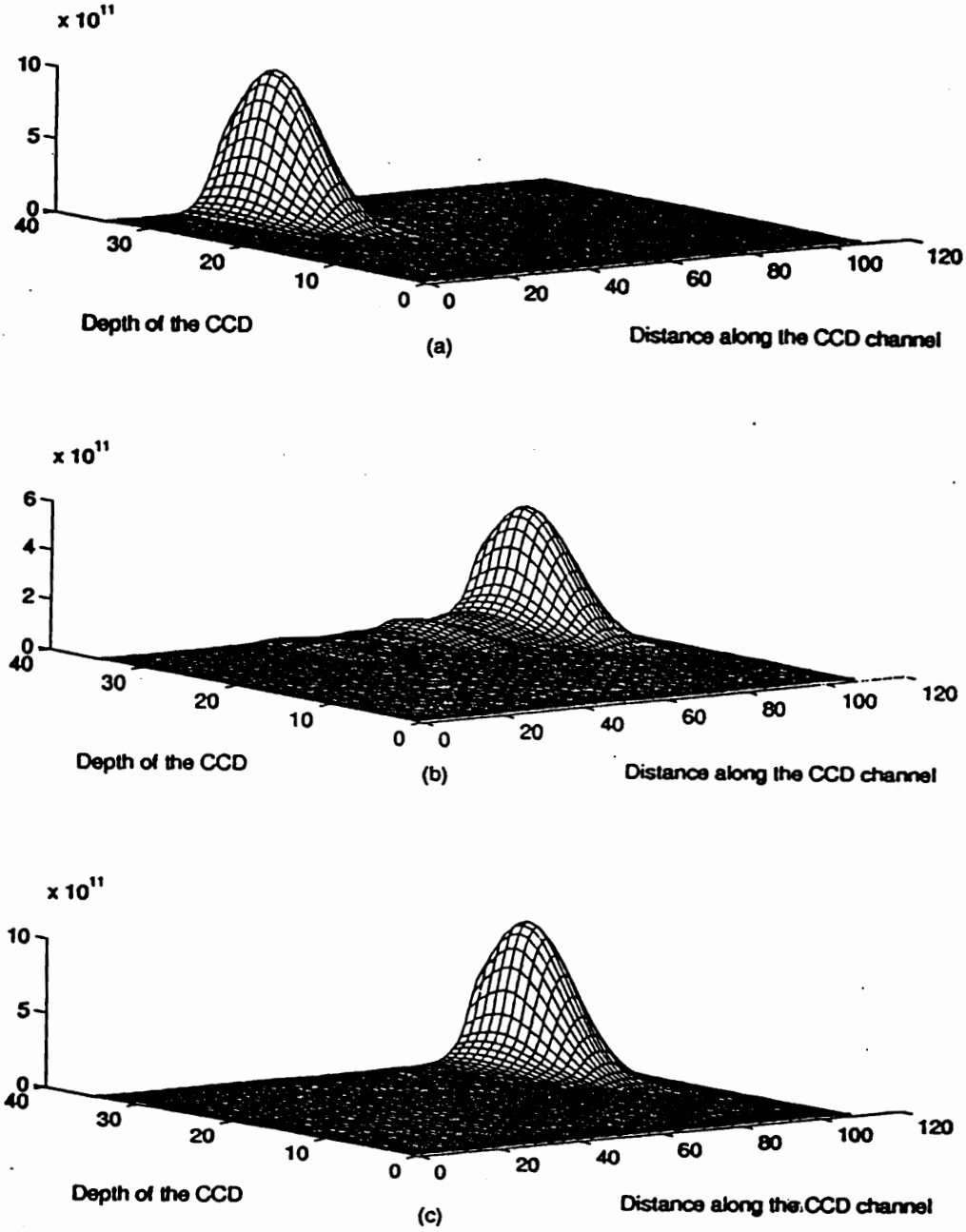

FIGURE 2. Time evolution of charges along a CCD. a) t=200 ps; b) t=400 ps; c) t=600 ps

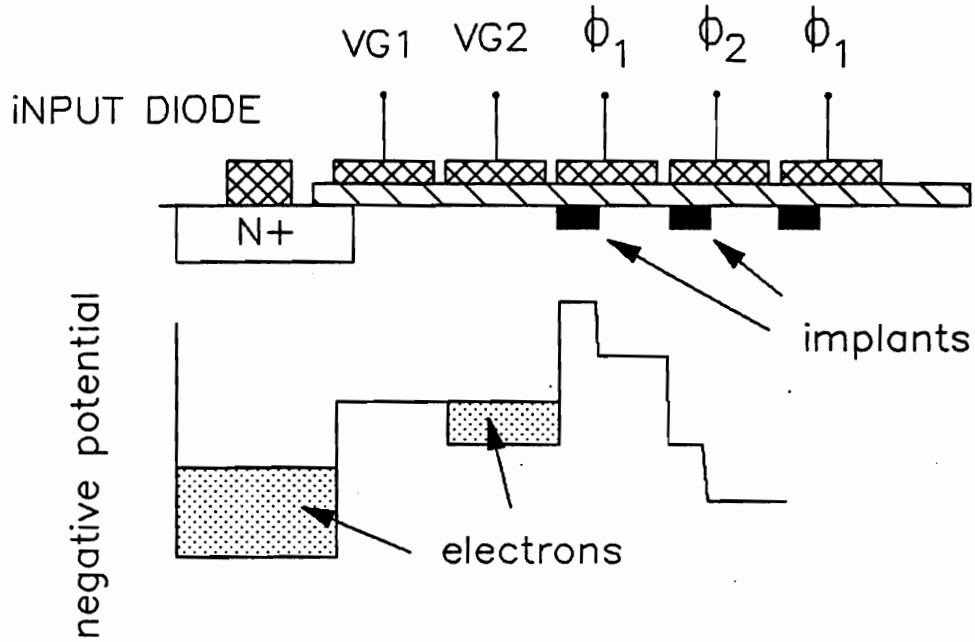

FIGURE 3. Input structure of a CCD.

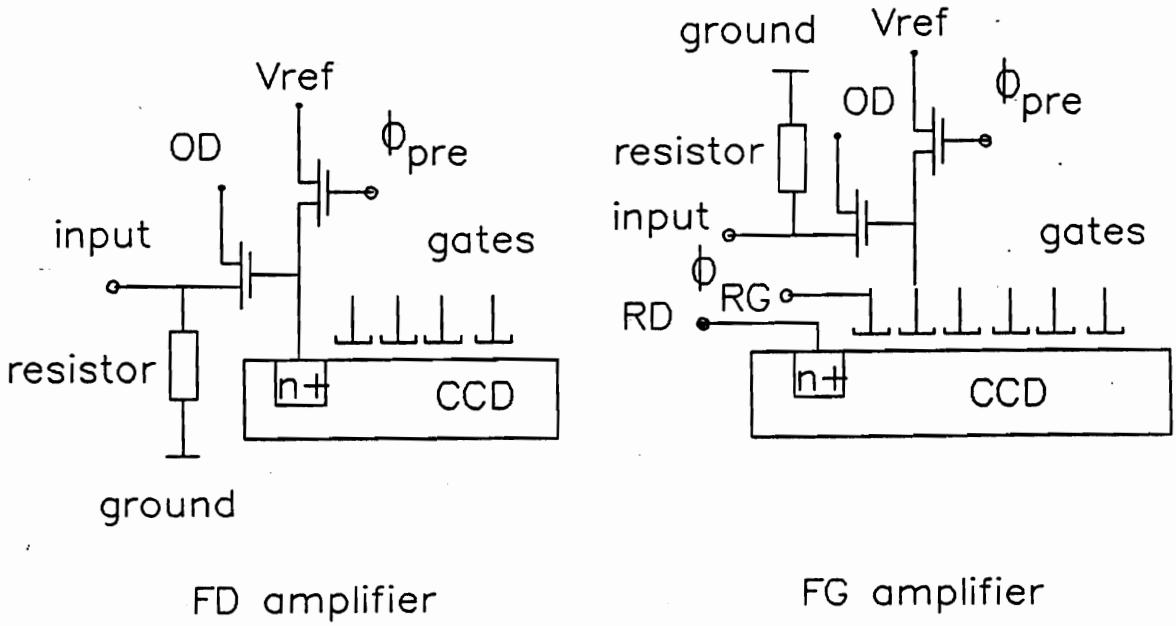

FIGURE 4. Output structures of a CCD.

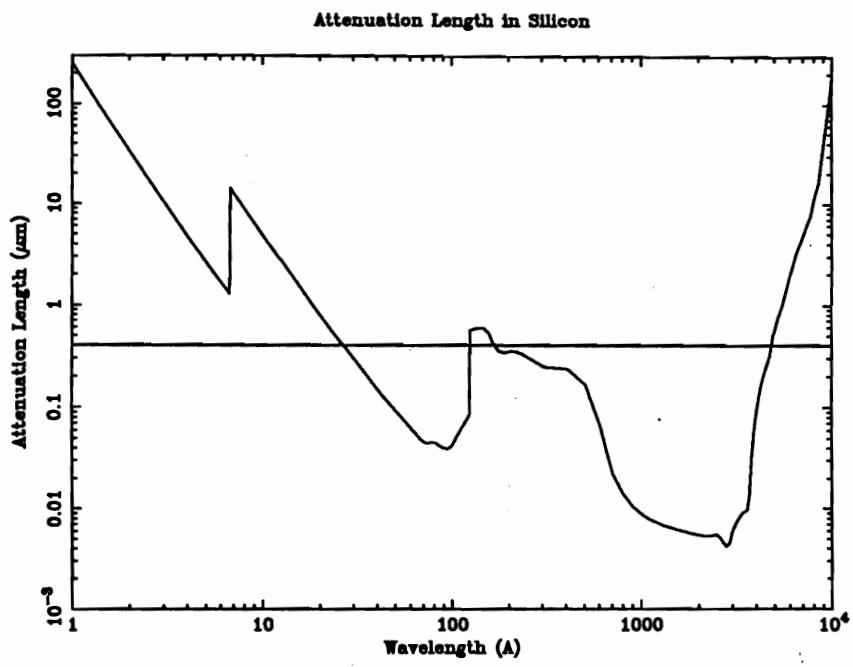

FIGURE 5. Attenuation length in silicon in the soft X-ray through near-infrared spectral range [8,9]. The polysilicon gates of front-illuminated devices, which are typically $\sim 0.4\mu m$ thick, are strongly absorbing at wavelengths for which the attenuation length is less than the gate thickness, viz., wavelengths ($\sim$30 Å $< \lambda <$ $\sim$4000 Å). Thin-gate and back-illuminated CCDs, with much thinner dead layers, offer improved detection efficiency in the soft X-ray and UV portions of the spectrum.

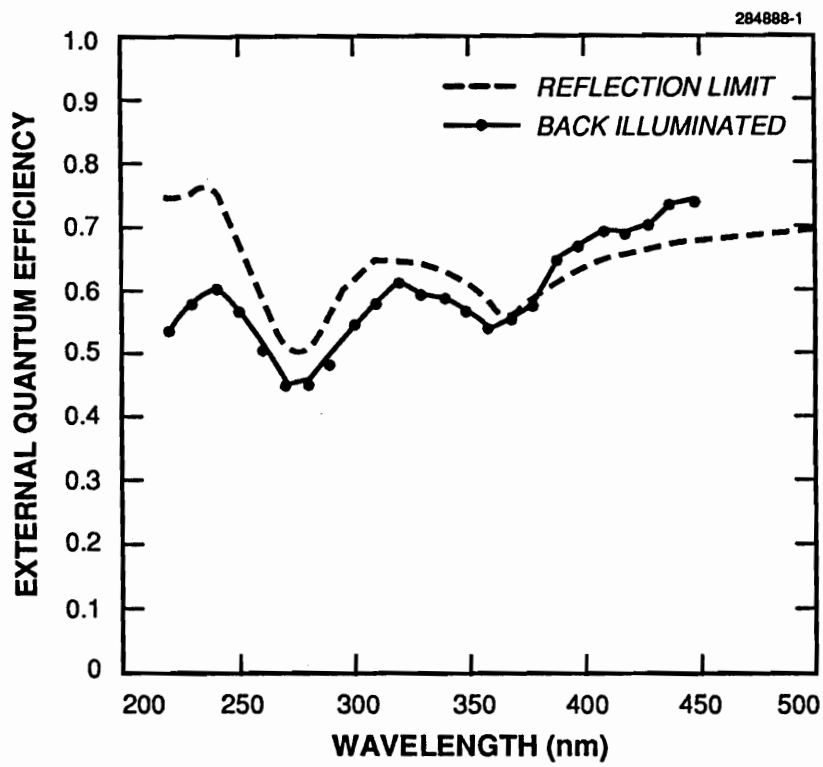

FIGURE 6. External quantum efficiency of back-illuminated CCD using an implanted and annealed back side. For comparison purposes, the external quantum efficiency of an ideal detector is shown, after modeling for the anti-reflection coating present on the back-illuminated detector.